ISSN 1070-4280, Russian Journal of Organic Chemistry, 2019, Vol. 55, No. 10, pp. 1591–1597. © Pleiades Publishing, Ltd., 2019.

Synthesis of Tetrazoles from Amines Mediated by New Copper Nanocatalyst

M. Ariannezhad[a], D. Habibi[a],* and S. Heydari[a]

[a] *Department of Organic Chemistry, Faculty of Chemistry, Bu-Ali Sina University, Hamedan, Iran*
**e-mail: davood.habibi@gmail.com*

Received May 11, 2019; revised August 17, 2019; accepted August 18, 2019

Abstract—New copper nanocatalyst was prepared by coating Fe_3O_4 magnetic nanoparticles with tetraethyl orthosilicate (TEOS), followed by functionalization with 3-chloropropyl(trimethoxy)silane and 4*H*-1,2,4-triazol-4-amine and complexation with copper(II) chloride. The new catalyst was characterized by various spectroscopic methods and was successfully used in the synthesis of 1-aryl-1*H*-tetrazoles by reaction of aromatic amines with sodium azide and triethyl orthoformate under solvent-free conditions at 100°C.

Keywords: Fe_3O_4 magnetic nanoparticles, 4*H*-1,2,4-triazole-4-amine, copper complex, aromatic amines, sodium azide, 1-aryl-1*H*-tetrazoles.

DOI: 10.1134/S1070428019100208

Tetrazole derivatives are used in biological and pharmaceutical industries [1–15], and the chemistry of tetrazoles has gained increasing attention since the early 1980s [2]. Among heterogeneous catalysts used for the synthesis of various tetrazoles, the application of nanocatalysts has received considerable attention in recent decades due to their unique surface and catalytic properties [16, 17]. The surface area to volume ratio increases with decrease in the radius of the sphere and vice versa. Therefore, as particle size decreases, a greater portion of atoms therein appear at the surface compared to those inside the particle. Thus, nanoparticles have a much greater surface area per unit volume compared with larger particles.

Reported syntheses of tetrazoles suffer from some disadvantages, such as low yield, long reaction times, harsh reaction conditions, low accessibility of starting materials, use of expensive and toxic reagents, and *in situ* generation of hydrazoic acid which is highly toxic and explosive [18, 19]. We tried to develop useful catalytic procedures that would have all possible benefits and advantages of the former methods without their disadvantages. For example, we reported the use of $ZnCl_2$ [20], $FeCl_3$–SiO_2 [21], natrolite zeolite [22], $ZnCl_2$/$AlCl_3$/silica (ZAS) [23], and ZnO [24] for the preparation of various tetrazole derivatives. Also, Fe_3O_4 magnetic particles were functionalized with 1,10-phenanthroline-5,6-diol, and the corresponding manganese complex was synthesized as a heterogeneous catalyst to be used for the one-pot three-component synthesis of various tetrazoles [25, 26].

The results of our studies showed that 5-arylamino-1*H*-tetrazole isomers can be obtained from arylcyanamides bearing an electron-withdrawing substituent on the aryl ring and that the reaction direction changed toward the formation of 1-aryl-5-amino-1*H*-tetrazole isomer as the electron-donating power of the substituent increased. We also found that the reactions with arylcyanamides having electron-donating groups on the aromatic ring were complete in a shorter time than the reactions with those containing electron-withdrawing substituents.

Now, we report a new heterogeneous copper nanocatalyst which was prepared by coating Fe_3O_4 magnetic nanoparticles with tetraethyl orthosilicate (Fe_3O_4/SiO_2), followed by functionalization with 3-chloropropyl(trimethoxy)silane and 4*H*-1,2,4-triazol-4-amine and complexation with copper(II) chloride. The new catalyst was characterized and applied to the synthesis of 1-aryl-1*H*-tetrazoles from various aromatic amines, sodium azide, and triethyl orthoformate under solvent-free conditions at 100°C.

The new copper nanocatalyst was synthesized according to Scheme 1 and was characterized by inductively coupled plasma (ICP) analysis, FT-IR, X-ray diffraction (XRD), energy dispersive X-ray spectroscopy (EDX), scanning electron microscopy (SEM), transmission electron microscopy (TEM),

Scheme 1.

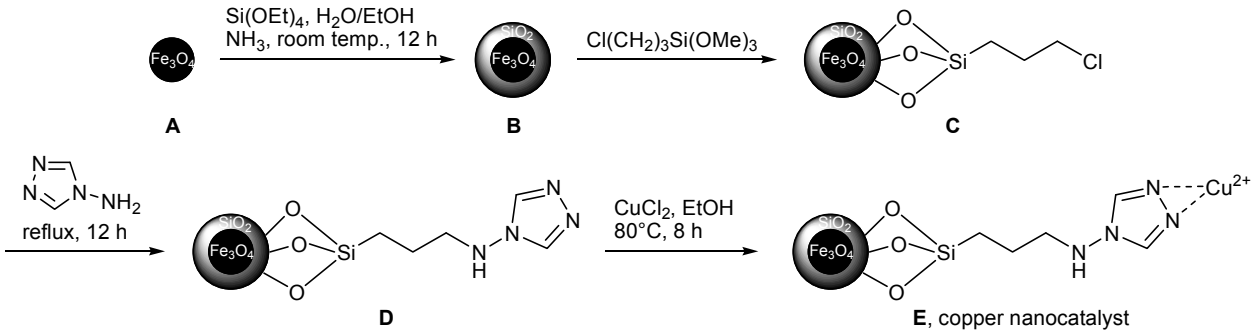

thermogravimetric–differential thermal analysis (TGA–DTA), and vibrating sample magnetometry (VSM).

The ICP analysis of the catalyst showed the Cu content of about 20.76%.

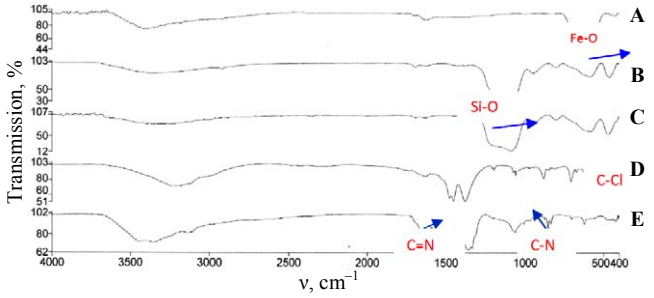

Fig. 1. FT-IR spectra of **A**, **B**, **C**, **D**, and **E**.

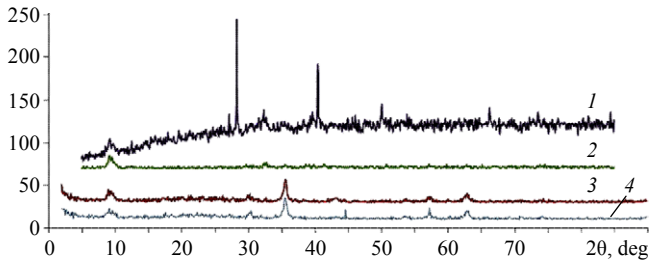

Fig. 2. XRD patterns of (*1*) Fe_3O_4/SiO_2 (**B**), (*2*) Fe_3O_4/SiO_2/CPTMS (**C**), (*3*) Fe_3O_4/SiO_2/CPTMS/AT (**D**), and (*4*) Fe_3O_4/SiO_2/CPTMS/AT/Cu (**E**).

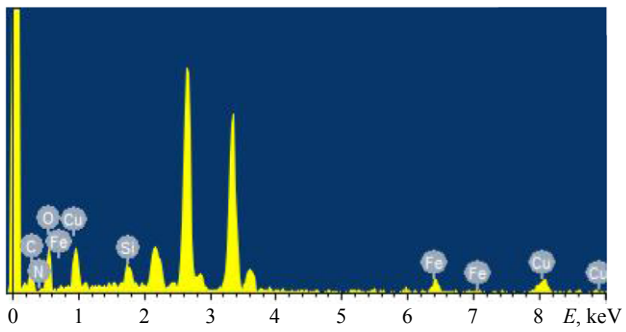

Fig. 3. EDX analysis of the catalyst.

Figure 1 shows the FT-IR spectra of **A**–**E**. The spectrum of **A** contains a basic characteristic peak at about 579 cm^{-1} which is attributed to Fe–O stretching vibrations. Curve **B** shows a broad band near 1086 cm^{-1} due to Si–O bonds. A new peak at 583 cm^{-1} in the spectrum of **C** indicates the presence of C–Cl bonds. Curve **D** displays two new peaks at 1338 and 1650 cm^{-1} corresponding to the triazole C–N and C=N bonds, respectively. Finally, the shift of the C=N band to 1627 cm^{-1} in the spectrum of the new catalyst (**E**) is related to copper coordination to the C=N nitrogen atom. Thus, comparison of the IR spectra of **A**–**E** confirms successful preparation of the Cu nanocatalyst.

The XRD pattern (Fig. 2, curve *1*) showed peaks at 2θ = 10, 30, 35, 45, 53, 57, 63, 74° which are consistent with the silica-coated magnetite nanoparticle structure. The new peaks at 2θ = 28, 40, 50, and 66° appeared in the X-ray powder pattern of **E** were attributed to Cu species (Fig. 2, curve *4*). The chemical composition of the Cu nanocatalyst was determined by EDX analysis (Fig. 3). The results confirm the presence of the anticipated elements in the structure of the catalyst, namely C, N, O, Si, Fe, and Cu. The morphology and the particle size of the Cu nanocatalyst were determined by SEM and TEM techniques (Figs. 4, 5). According to the obtained images, the nanocatalyst particle size is in the nanometer range (between 44.28 and 63.24 nm).

The thermogravimetric analysis curves of the catalyst showed weight loss due to thermal decomposition of the organic material (Fig. 6). The catalyst showed about three weight loss steps in the temperature ranges of 140, 175, and 235°C, respectively. The initial weight loss at 140°C is probably due to the residual water, the second step at 175°C is attributed to the thermal decomposition of the complex, and the third step is probably due to thermal decomposition of the aminotriazole and (propyl)silane moieties.

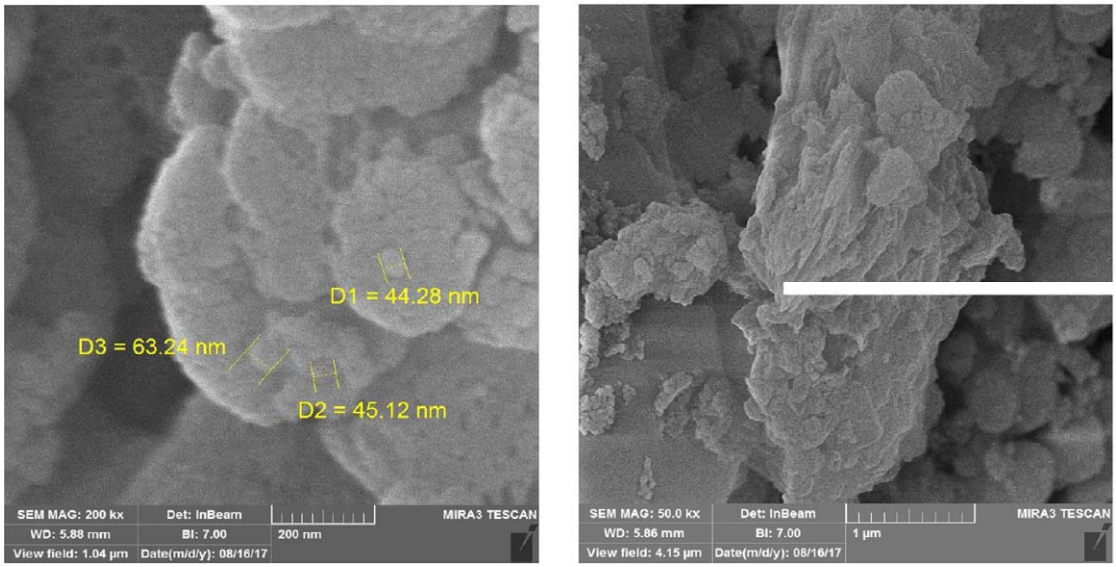

Fig. 4. SEM images of the catalyst.

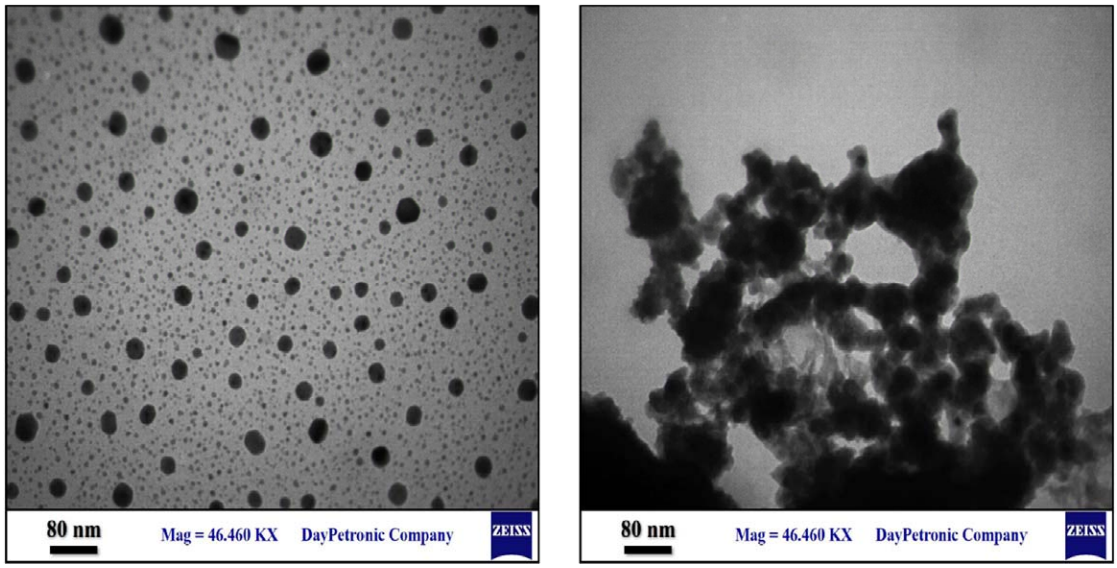

Fig. 5. TEM images of the catalyst.

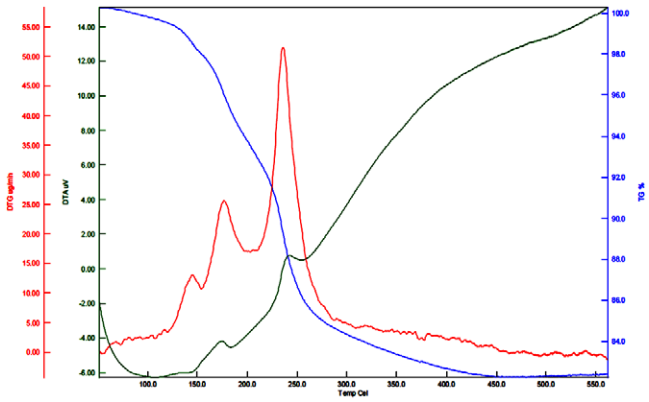

Fig. 6. TGA–DTA patterns of the catalyst in a nitrogen atmosphere.

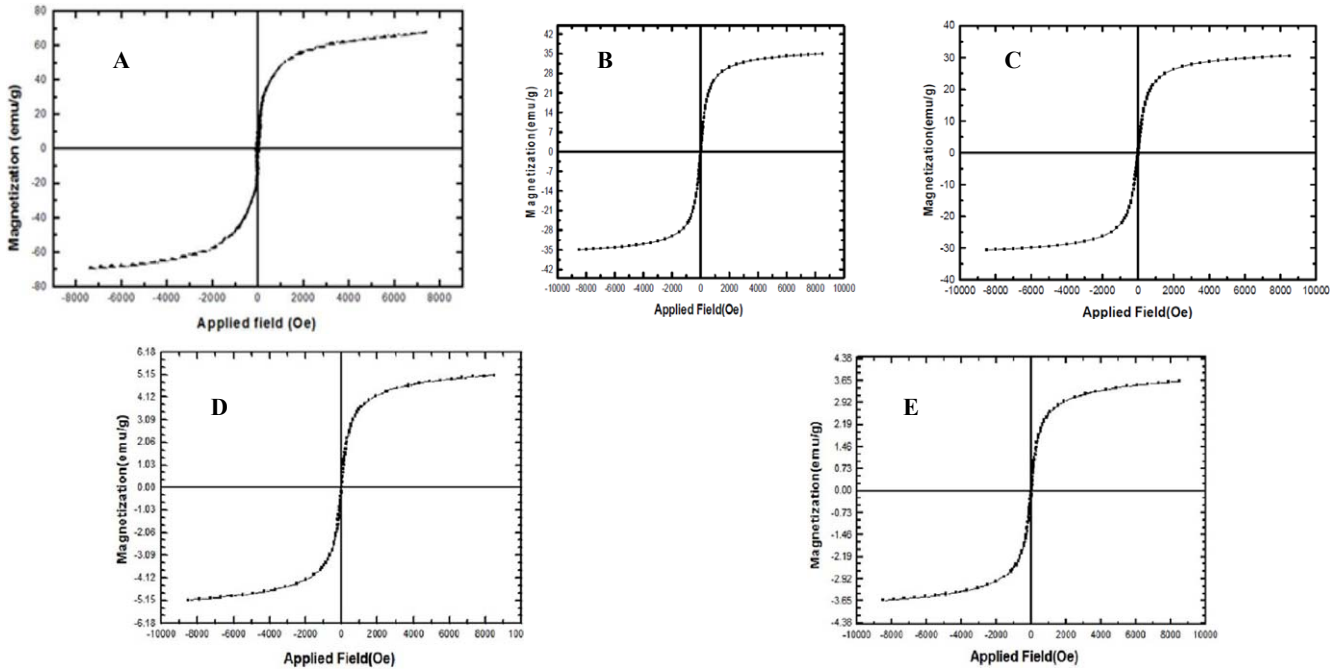

Fig. 7. VSM analyses of **A**–**E**.

The VSM analyses of **A**–**E** were performed in order to demonstrate and compare their magnetic properties (Fig. 7). As can be seen, all five compounds have magnetic properties which decrease in going from **A** to **E** (65, 35, 30, 5.15, and 3.65 emu/g, respectively). This can be explained assuming probable reduction in dipole–dipole interactions between magnetic nanoparticles after modification and complexation which make them coated to a greater extent.

The new catalyst was tested in the synthesis of 1-aryl-1*H*-tetrazoles **2a**–**2j** by reaction of aromatic amines **1a**–**1j** with sodium azide and triethyl orthoformate (Scheme 2). The reaction conditions were optimized using the reaction of 4-nitroaniline with sodium azide and $HC(OEt)_3$ as model by varying the catalyst amount, solvent, and temperature (Tables 1–3). The best result was obtained using equimolar amounts (2 mmol) of the reactants and 50 mg of copper nanocatalyst at 100°C in the absence of a solvent. The optimized conditions were then applied to the reactions with other substituted anilines, and the corresponding 1-aryl-1*H*-tetrazoles were obtained with good to excellent yields (Table 4).

1-Aryl-1*H*-tetrazoles **2a**–**2j** were reported previously. The products were identified by comparing their physical and spectroscopic data with those given in the literature. Their structures were in agreement with the IR and NMR spectra. In the IR spectra of all products, no sharp NH_2 peak typical of initial anilines was observed in the region 3300–3500 cm^{-1}.

Scheme 3 outlines a plausible mechanism for the formation of tetrazoles in the described reaction. Being a Lewis acid, the catalyst is likely to add to the oxygen atom of ethoxy group of $HC(OEt)_3$, which facilitates nucleophilic attack of the amino nitrogen atom on the central carbon atom of the ortho ester. Next follow successive elimination of two ethanol molecules, nucleophilic attack of azide anion, and cyclization to form the final product.

The reusability of the Cu nanocatalyst was studied in the model reaction. The catalyst was separated from the reaction mixture by filtration after the first run,

Scheme 2.

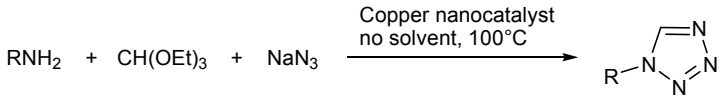

1a–1j **2a–2j**

R = Ph (**a**), 2,4-$Me_2C_6H_3$ (**b**), 4-MeC_6H_4 (**c**), 4-$MeOC_6H_4$ (**d**), $_4$-$MeC(O)C_6H_4$ (**e**), 4-BrC_6H_4 (**f**), 2-ClC_6H_4 (**g**), 4-ClC_6H_4 (**h**), 4-$O_2NC_6H_4$ (**i**), 3-$F_3CC_6H_4$ (**j**).

Scheme 3.

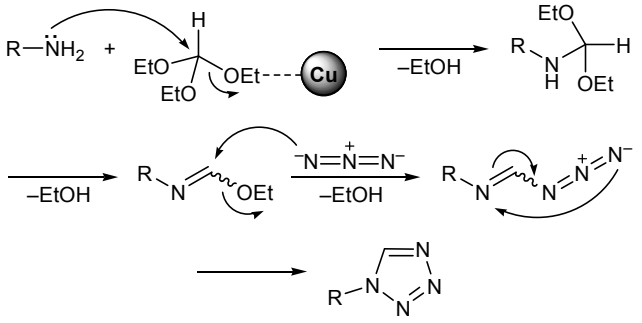

washed with ethanol, dried under reduced pressure, and reused for the next run under the same conditions. The yields of tetrazole **2i** in five successive runs were 93, 91, 88, 85, and 82%, respectively. Thus, the new catalyst can be reused up to five times without significant loss of activity.

In summary, we have prepared a new heterogeneous copper nanocatalyst from silica-coated Fe_3O_4 nanoparticles modified with 3-chloropropyl(trimethoxy)silane and 4*H*-1,2,4-triazol-4-amine and demonstrated its high efficiency in the solvent-free synthesis of 1-aryl-1*H*-tetrazoles from substituted anilines, sodium azide, and triethyl orthoformate at 100°C.

EXPERIMENTAL

The IR spectra were recorded on a Perkin–Elmer GX Fourier transform infrared spectrometer. The NMR spectra were recorded on a Jeol FT NMR 90 spectrometer. The TEM images were recorded on a Zeiss-EM10C-80 KV transmission electron microscope, and the SEM images were recorded on a Philips XL-30 scanning electron microscope. The XRD measurements were done with a Bruker D8 Advance powder diffractometer (Cu K_α radiation, λ = 1.54 Å). The size distributions were measured with a Malvern Zetasizer Nano-ZS-90 (ZEN 3600) instrument. The ICP measurements of the metal content were performed using a Perkin Elmer ICP/6500 instrument. Magnetic measurements were carried out at room temperature using an Iranian Meghnatis Daghigh Kavir Co. Vibrating Sample Magnetometer (VSM). Chemicals and solvents were purchased from Merck and Sigma-Aldrich and used without further purification.

Preparation of copper nanocatalyst. A mixture of $FeCl_3 \cdot 6H_2O$ (11.44 g) and $FeCl_2 \cdot 4H_2O$ (4.3 g) was dissolved in water (100 mL), and the solution was stirred for 0.5 h at 80°C. A 37% aqueous ammonia solution was then added dropwise with vigorous stirring, and a black solid separated when pH reached a value of 10. The mixture was heated for 0.5 h at 70°C, and the black magnetic solid (Fe_3O_4 magnetic nanoparticles, **A**) was filtered off, washed with water, and dried at 80°C for 12 h. A 0.2-g sample of Fe_3O_4 MNPs was dispersed in a mixture of ethanol and distilled water (250 mL, 4:1 by volume) and aqueous ammonia (3 mL) under ultrasonication. Tetraethyl orthosilicate (2 mL) was then slowly added dropwise, and the mixture was stirred for 6 h. The product (**B**) was separated by centrifugation, washed with water and ethanol for several times, and dried under reduced pressure. 3-Chloropropyl(trimethoxy)silane (1.0 mL, 5 mmol) was dissolved in anhydrous toluene (100 mL), Fe_3O_4/SiO_2 (1.0 g) was added, and the mixture was stirred for 18 h at 60°C. The resulting magnetic solid (**C**) was separated using a strong magnet, washed with toluene, and dried under reduced pres-

Table 1. Effect of the catalyst amount on the yield of **2i**[a]

Catalyst, mg	Yield, %
10	Traces
20	35
30	53
40	73
50	93

[a] Reaction conditions: **1i**, 2 mmol; NaN_3, 2 mmol; $HC(OEt)_3$, 2 mmol; no solvent, 100°C, 2 h.

Table 2. Effect of solvent on the yield of **2i**[a]

Solvent	Yield, %
H_2O	Traces
EtOH	18
DMF	74
Toluene	42
DMSO	61
None	93

[a] Reaction conditions: **1i**, 2 mmol; NaN_3, 2 mmol; $HC(OEt)_3$, 2 mmol; catalyst, 50 mg; solvent, 5 mL, 100°C, 2 h.

Table 3. Effect of temperature on the yield of **2i**[a]

Temperature, °C	Yield. %
18–25	21
40	42
80	71
100	93

[a] Reaction conditions: **1i**, 2 mmol; NaN_3, 2 mmol; $HC(OEt)_3$, 2 mmol; catalyst, 50 mg; no solvent, 2 h.

Table 4. Synthesis of tetrazoles **2a**–**2j**

Initial compd. no.	Product no.	Reaction time, min	Yield, %	mp, °C	
				found	reported
1a	**2a**	80	90	63–66	64–65
1b	**2b**	100	82	132–134	133–135
1c	**2c**	90	92	93–95	94–95
1d	**2d**	100	91	113–115	114–115
1e	**2e**	110	87	174–177	177
1f	**2f**	180	75	176–180	183–185
1g	**2g**	100	85	127–131	127–131
1h	**2h**	180	86	156–158	157–158
1i	**2i**	120	93	199–203	201–202
1j	**2j**	115	82	124–128	125–127

sure. A mixture of 4*H*-1,2,4-triazol-4-amine (0.42 g, 5 mmol) and potassium carbonate (0.69 g, 5 mmol) in toluene (60 mL) was added to 0.1 g of **C**, and the mixture was refluxed for 12 h. The product (**D**) was separated with a strong magnet, washed repeatedly with ethanol and water, and dried under reduced pressure. A 0.1-g sample of **D** was added to a suspension of copper(II) chloride (0.85 g, 5 mmol) in ethanol, and the mixture was vigorously stirred for 8 h at 80°C. The resulting copper nanocatalyst (**E**) was separated with a strong magnet, washed with ethanol, and air-dried.

1-Aryl-1*H*-tetrazoles 2a–2j (*general procedure*). A mixture of 2 mmol of aromatic amine **1a**–**1j**, 0.13 g (2 mmol) of sodium azide, 0.296 g (2 mmol) of triethyl orthoformate, and 50 mg of the copper nanocatalyst was stirred at 100°C until no further progress in the conversion was observed according to the TLC data. The mixture was allowed to cool down to room temperature, the catalyst was separated by strong magnet, the mixture was poured onto ice, and the organic layer was extracted with ethyl acetate (2×20 mL). The combined extracts were dried over anhydrous $MgSO_4$, filtered, and evaporated, and the residue was recrystallized from ethyl acetate–hexane (1:10). The yields and melting points of tetrazoles **2a–2j** are given in Table 4.

1-Phenyl-1*H*-tetrazole (2a). IR spectrum (KBr), ν, cm^{-1}: 3051, 2925, 2854, 1678, 1660, 1585, 1487, 1448, 1316, 1279, 1227, 1209, 1171, 1153, 1076, 986, 899, 806, 765, 754, 694, 619, 593. ^{1}H NMR spectrum (90 MHz, $CDCl_3$), δ, ppm: 8.27 s (1H), 6.98–7.60 m (5H).

1-(2,4-Dimethylphenyl)-1*H*-tetrazole (2b). IR spectrum (KBr), ν, cm^{-1}: 3157, 3015, 2876, 1665, 1496, 1302, 1206, 1036, 815, 561. ^{1}H NMR spectrum (90 MHz, $CDCl_3$), δ, ppm: 8.39 s (1H), 6.96 m (3H), 2.29 s (6H).

1-(4-Methylphenyl)-1*H*-tetrazole (2c). IR spectrum (nujol), ν, cm^{-1}: 3027, 2914, 2857, 1672, 1608, 1587, 1521, 1506, 1408, 1313, 1217, 1202, 1174, 1110, 1040, 985, 938, 821, 738, 716, 644, 578. ^{1}H NMR spectrum (90 MHz, $CDCl_3$), δ, ppm: 8.16 s (1H), 7.27–6.92 m (4H), 2.30 s (3H).

1-(4-Methoxyphenyl)-1*H*-tetrazole (2d). IR spectrum (nujol), ν, cm^{-1}: 1667, 1504, 1464, 1243, 1034, 826. ^{1}H NMR spectrum (90 MHz, $CDCl_3$), δ, ppm: 8.05 s (1H), 6.88 m (4H), 3.7 s (3H).

1-[4-(1*H*-Tetrazol-1-yl)phenyl]ethan-1-one (2e). IR spectrum (KBr), ν, cm^{-1}: 3059, 2996, 2962, 1674, 1603, 1589, 1503, 1483, 1411, 1359, 1324, 1303, 1271, 1211, 1186, 1172, 997, 957, 910, 841, 815, 734, 685, 635, 590. ^{1}H NMR spectrum (90 MHz, $CDCl_3$), δ, ppm: 8.29 s (1H), 8.00–7.09 m (4H), 2.59 s (3H).

1-(4-Bromophenyl)-1*H*-tetrazole (2f). IR spectrum (KBr), ν, cm^{-1}: 3527, 3151, 3045, 2855, 1660, 1589, 1575, 1483, 1402, 1312, 1291, 1224, 1206, 1073, 1008, 827. ^{1}H NMR spectrum (90 MHz, $CDCl_3$), δ, ppm: 8.07 s (1H), 7.40 d (2H, J = 8.6 Hz), 6.90 d (2H, J = 8.6 Hz).

1-(2-Chlorophenyl)-1*H*-tetrazole (2g). IR spectrum (KBr), ν, cm^{-1}: 2998, 2866, 1666, 1583, 1502, 1475, 1454, 1439, 1376, 1309, 1264, 1207, 1132, 1058, 1039, 1000, 935, 825, 752, 702, 657. ^{1}H NMR spectrum (90 MHz, $CDCl_3$), δ, ppm: 8.07 s (1H), 7.44–7.10 m (4H).

1-(4-Chlorophenyl)-1*H*-tetrazole (2h). IR spectrum (KBr), ν, cm^{-1}: 2925, 1663, 1581, 1488, 1405, 1311, 1292, 1226, 1205, 1172, 1090, 1006, 984, 829,

810, 700, 650, 631, 570. ^{1}H NMR spectrum (90 MHz, $CDCl_3$), δ, ppm: 8.09 s (1H), 7.28 d (2H, J = 6.7 Hz), 6.96 d (2H, J = 6.7 Hz).

1-(4-Nitrophenyl)-1*H*-tetrazole (2i). IR spectrum (nujol), ν, cm^{-1}: 3105, 2985, 1660, 1599, 1579, 1508, 1396, 1344, 1313, 1301, 1238, 1205, 1173, 1107, 989, 958, 861, 845, 784, 750, 708, 687, 642. ^{1}H NMR spectrum (90 MHz, acetone-d_6), δ, ppm: 8.52 s (1H), 8.23 d (2H, J = 8.8 Hz), 7.57 d (2H, J = 8.8 Hz).

1-(3-Trifluoromethylphenyl)-1*H*-tetrazole (2j). IR spectrum (KBr), ν cm^{-1}: 3275, 3220, 3140, 3005, 2981, 2940, 2840, 1620, 1585. ^{1}H NMR spectrum (90 MHz, DMSO-d_6), δ, ppm: 8.19 s (1H), 7.60–7.20 m (4H).

ACKNOWLEDGMENTS

The authors are grateful to the Bu-Ali Sina University, Hamedan, Iran, for the financial support of this work.

CONFLICT OF INTEREST

The authors declare no conflict of interest.

REFERENCES

1. Wittenberger, S.J., *Org. Prep. Proced. Int*., 1994, vol. 26, p. 499. https://doi.org/10.1080/00304949409458050
2. Butler, R.N., *Comprehensive Heterocyclic Chemistry II*, Katritzky, A.R., Rees, C.W., and Scriven, E.F.V., Eds., Oxford: Pergamon, 1996, vol. 4, p. 621. https://doi.org/10.1016/B978-008096518-5.00095-2
3. Herr, R.J., *Bioorg Med. Chem*., 2002, vol. 10, p. 3379. https://doi.org/10.1016/S0968-0896(02)00239-0
4. Peet, N.P., Baugh, L.E., Sundler, S., Lewis, J.E., Matthews, E.H., Olberding, E.L., and Shah, D.N., *J. Med. Chem*., 1986, vol. 29, p. 2403. https://doi.org/10.1021/jm00161a045
5. Girijavallabhan, V.M., Pinto, P.A., Genguly, A.K., and Versace, R.W., EP Patent no. 274867, 1988; *Chem. Abstr*., 1989, vol. 110, no. 23890.
6. Akimoto, H., Ootsu, K., and Itoh, F., EP Patent no. 530537, 1993; *Chem. Abstr*., 1993. vol. 119, no. 226417; Mitch, C.H. and Quimby, S.J., WO Patent Appl. Pub. no. 98/51312, 1998; *Chem. Abstr*., 1998, vol. 130, no. 13997.
7. Jursic, B.S., and LeBlanc, B.W., *J. Heterocycl. Chem*., 1998. vol. 35, p. 405. https://doi.org/10.1002/jhet. 5570350224
8. John, E.O., Kirchmeier, R.L., and Shreeve, J.M., *Inorg. Chem*., 1989, vol. 28, p. 4629. https://doi.org/10.1039/C4RA06463A
9. Zhao-Xu, C. and Heming, X., *Int. J. Quantum Chem*., 2000, vol. 79, p. 350. https://doi.org/10.1007/s10973-014-3643-4
10. Ek, F., Wistr, L.-G., and Frejd, T., *Tetrahedron*, 2003, vol. 59, p. 6759. https://doi.org/10.1016/S0040-4020(03)00818-4
11. Flippin, L.A., *Tetrahedron Lett*., 1991, vol. 32, p. 6857. https://doi.org/10.1016/0040-4039(91)80425-6
12. Rhonnstad, P. and Wensbo, D., *Tetrahedron Lett*., 2002, vol. 43, p. 3137. https://doi.org/10.1016/S0040-4039(02)00490-2
13. Modarresi-Alam, A.R., Khamooshi, F., Rostami-zadeh, M., Kieykha, H., Nasrollahzadeh, M., Bijanzadeh, H.R., and Kleinpeter, E., *J. Mol. Struct*., 2007, vol. 841, p. 61. https://doi.org/10.1016/j.molstruc.2006.11.058
14. Sandmann, G., Schneider, C., and Böger, P., *Z. Naturforsch., Teil C*, 1996, vol. 51, p. 534.
15. Ponec, V. and Bond, G.C., *Catalysis by Metals and Alloys*, Amsterdam: Elsevier: 1995.
16. Lim, C.W. and Lee, I.S., *Nano Today*, 2010, vol. 5, p. 412. https://doi.org/10.1016/j.nantod.2010.08.008
17. Butler, R.N., *Adv. Heterocycl. Chem*., 1977, vol. 21, p. 323. https://doi.org/10.1016/S0065-2725(08) 60735-7
18. Jin, T., Kitahara, F., Kamijo, S., and Yamamoto, Y., *Tetrahedron Lett*., 2008, vol. 49, p. 2824. https://doi.org/10.1016/j.tetlet.2008.02.115
19. Habibi, D., Nasrollahzadeh, M., Faraji, A., and Bayat, Y., *Tetrahedron*, 2010, vol. 66, p. 3866. https://doi.org/10.1016/j.tet.2010.03.003
20. Habibi, D. and Nasrollahzadeh, M., *Synth. Commun*., 2010, vol. 40, p. 3159. https://doi.org/10.1080/00397910903370683
21. Nasrollahzadeh, M., Habibi, D., Shahkarami, Z., and Bayat, Y., *Tetrahedron*, 2009, vol. 65, p. 10715. https://doi.org/10.1016/j.tet.2009.10.029
22. Habibi, D. and Nasrollahzadeh, M., *Monatsh. Chem*., 2012, vol. 143, p. 925. https://doi.org/10.1007/s00706-011-0670-8
23. Habibi, D., and Nasrollahzadeh, M., *Synth. Commun*., 2012, vol. 41, p. 2023. https://doi.org/10.1080/00397911.2010.548620
24. Habibi, D., Heydari, S., Afsharfarnia, M., and Rostami, Z., *Appl. Organomet. Chem*., 2017, vol. 31, p. e3826. https://doi.org/10.1002/aoc.3826
25. Habibi, D., Heydari, S., Gil, A., Afsharfarnia, M., Faraji, A., Karamian, R., and Asadbegy, M., *Appl. Organomet. Chem*., 2018, vol. 32, p. e4005. https://doi.org/10.1002/aoc.4005
26. Ariannezhad, M., Habibi, D., and Heydari, S., *Polyhedron*, 2019, vol. 160, p. 170. https://doi.org/10.1016/j.poly.2018.12.037